Assessment of soil features on the growth of environmental nontuberculous mycobacterial isolates from Hawai'i

* Cody M. Glickman [a]
* Ravleen Virdi [a]
Nabeeh A. Hasan, PhD [a]
L. Elaine Epperson, PhD [a]
Leeza Brown [b]
Stephanie N. Dawrs [a]
James L. Crooks [c]
Edward D. Chan [d,e,f]
Michael Strong, PhD [a]
Stephen T. Nelson, PhD [b]
[1]Jennifer R. Honda, PhD [a]

[a] Center for Genes, Environment and Health, National Jewish Health, Denver, Colorado, USA
[b] Department of Geological Sciences, Brigham Young University, Provo, Utah, USA
[c] Division of Biostatistics and Bioinformatics, National Jewish Health, Denver, Colorado, USA
[d] Medicine and Academic Affairs, National Jewish Health, Colorado, USA
[e] Division of Pulmonary Sciences and Critical Care Medicine, University of Colorado Anschutz Medical Campus, Aurora, Colorado, USA
[f] Department of Medicine, Rocky Mountain Regional Veterans Affairs Medical Center, Denver, Colorado, USA.

* Cody M. Glickman and Ravleen Virdi contributed equally to this work. Author order was determined alphabetically.

[1] Corresponding Author

Jennifer R. Honda, PhD; Mailing Address: National Jewish Health, 1400 Jackson St., Neustadt Building D504, Denver, CO 80206 U.S.A.; Office: 303-398-1015; Fax: 303-270-2185; U.S.A. (email: hondaJ@njhealth.org)

Running Title: Soil features that contribute to NTM growth

Keywords: nontuberculous mycobacteria, soil minerals, Hawai'i

ABSTRACT

Environmental nontuberculous mycobacteria (NTM) with the potential to cause opportunistic lung infections can reside in soil. This might be particularly relevant in Hawai'i, a geographic hot spot for NTM infections and whose soil composition differs from many other areas of the world. Soil components are likely to contribute to NTM prevalence in certain niches, as food sources or attachment scaffolds, but the particular types of soils, clays, and minerals that impact NTM growth are not well-defined. Hawai'i soil and chemically weathered rock (*a.k.a.*, saprolite) samples were examined to characterize the microbiome and quantify 11 mineralogical features as well as soil pH. Machine learning methods were applied to identify important soil features influencing the presence of NTM. Next, these features were directly tested *in vitro* by incubating synthetic clays and minerals in the presence of *Mycobacteroides abscessus* and *Mycobacterium chimaera* isolates recovered from the Hawai'i environment and changes in bacterial growth were determined. Of the components examined, synthetic gibbsite, a mineral form of aluminum hydroxide, inhibited the growth of both *M. abscessus* and *M. chimaera*, while other minerals tested showed differential effects on each species. For example, *M. abscessus* (but not *M. chimaera*) growth was significantly higher in the presence of hematite, an iron oxide mineral. In contrast, *M. chimaera* (but not *M. abscessus*) counts were significantly reduced in the presence of birnessite, a manganese containing mineral. These studies shed new light on the mineralogic features that promote or inhibit the presence of Hawai'i NTM in Hawai'i soil.

54 **IMPORTANCE**

55

56 Globally and in the United States, the prevalence of nontuberculous mycobacterial (NTM)
57 pulmonary disease - a potentially life-threatening, but under-diagnosed chronic illness – is
58 prominently rising. While NTM are ubiquitous in the environment including soil, the specific
59 soil components that promote or inhibit NTM growth have not been elucidated. We hypothesized
60 that NTM-culture positive soil contains minerals that promote NTM growth *in vitro*. Because
61 Hawai'i is a hot spot for NTM and a unique geographic archipelago, we examined the
62 composition of Hawai'i soil and identified individual clay, iron, and manganese minerals
63 associated with NTM. Next, individual components were evaluated for their ability to directly
64 modulate NTM growth in culture. In general, gibbsite and some manganese oxides were shown
65 to decrease NTM, whereas iron containing minerals were associated with higher NTM counts.
66 These data provide new information to guide future analyses of soil-associated factors impacting
67 persistence of these soil bacteria.

68 **INTRODUCTION**

69

70 Natural and man-made environments harbor potentially disease-causing species of
71 nontuberculous mycobacteria (NTM) (1). The NTM species responsible for human lung
72 infections are thought to be influenced by the specific environmental source exposures and the
73 NTM species diversity within these environmental niches. While water-associated biofilms
74 contain potentially disease-causing NTM, a variety of NTM species have also been discovered in
75 soil (2-4). Prior studies have shown that potting soil can be a reservoir for clinically relevant
76 mycobacteria (4). In Japan, residential soil from patients with pulmonary NTM infections were
77 demonstrated to harbor NTM that were genetically related to patients' respiratory NTM isolates
78 and that soil was a source of the patients' polyclonal and mixed *Mycobacterium avium* complex
79 infections (5, 6). In the United States (U.S.), Hawai'i has the highest prevalence of NTM lung
80 infections with almost four times higher NTM infection rates than the national average in a
81 survey among older adults (7). In prior work (8), we reported the presence of clinically relevant
82 slow-growing mycobacteria (SGM) including *Mycobacterium chimaera*, *Mycobacterium*
83 *marseillense*, and *Mycobacterium intracellulare* in Hawai'i soil samples, in addition to rapid-
84 growing mycobacteria (RGM) including *Mycolicibacterium septicum* and *Mycolicibacterium*
85 *alvei*.

86

87 The breadth of NTM species diversity in soil is likely driven by the proportion and composition
88 of minerals and nutrients in that particular soil sample. For example, higher amounts of metals
89 such as copper, and cations such as sodium, have been shown to be significant predictors for
90 NTM infection in the U.S. (9). Prior studies from Queensland, Australia have shown soil

containing nutrients such as nitrate or having low pH predicted the presence of RGM, including *Mycolicibacterium fortuitum* and *Mycobacteroides chelonae* (10). Yet, soil components such as natural rock, sand, or clay may also impact NTM presence and diversity. A study by Lipner *et al.* reported increasing clay concentrations as protective against NTM, while increasing silt concentrations was associated with NTM infection (11). In this same study and another, higher manganese concentration was associated with disease prevalence (9, 11). Thus, variable soil characteristics and components may either inhibit or promote NTM growth in soil.

In the current study, we performed microbiome and mineral/chemical analyses on a set of Hawai'i soil samples and tested the impact of particular clays and chemicals on the *in vitro* growth of native NTM species recovered from the Hawai'i environment. Since almost all of the rock underlying Hawai'i ecosystems is oceanic basalt, comprised of volcanic rock with limited variations in composition (12), the characteristics associated with the presence of NTM in Hawai'i soil may significantly vary from what has been described so far.

MATERIAL AND METHODS

Soil samples and NTM isolates used in this study

In 2012, 65 different soil samples were collected from locations across Oahu, Kauai, Hawai'i Island, Molokai, and Maui and NTM culture diversity from these samples were previously reported (8). A subset of 55 samples were used for downstream processing due to missing data and their collection sites were plotted in **Figure 1** based on global positioning system coordinates. Average rainfall of the sites ranged from less than 1,000 mm/year to 2,000 mm/year. Of note, this study did not consider soil types categorized by the USDA classification system. Of these soils, 13/65 (20 %) were NTM culture positive. To assess the impact of soil minerals and components on NTM growth *in vitro*, two environmental Hawai'i NTM isolates were tested in the *in vitro* studies detailed herein including: 12-45-Sw-A-1 *Mycobacteroides abscessus* subsp. *abscessus* isolated from an Oahu household kitchen sink biofilm and 12-56-S-1-1 *M. chimaera* isolated from an Oahu household garden soil sample *(8). M. avium* subsp. *hominissuis* H87 isolated from an indoor sink faucet was also tested (13).

Microbiome Analysis

Of the 55 soil samples, a subset including eight NTM culture positive and ten NTM culture negative soils were subjected to microbiome profiling. DNA was obtained using the PowerSoil TM DNA Isolation Kit from MoBio Labs, Inc (14). Small subunit ribosomal sequencing reads were generated on an Ion Torrent Personal Genome Machine. The V4 region of the 16S rRNA gene was amplified from total extracted DNA using the following primers: 515F, 5′-GTGCCAGCMGCCGCGGTAA-3′; 806R, 5′-GGACTA CHVGGGTWTCTAAT-3′ sequencing

reads were processed through Dada2 (version 1.6.0) to infer sequence variants in R (version 3.4.4) (15, 16). The Dada2 processing pipeline was adjusted to operate on Ion Torrent semiconductor data by adjusting the homopolymer gap penalty to -1 and increasing the band size parameter to 32 per instructions from the package creators. In addition to the Hawai'i samples, the sequencing run included a no template control (NTC) to account for spurious amplification during the library preparation. Following sequence variant tabulation with Dada2, counts that remained in the NTC were deducted from the soil samples. The resulting samples had a mean of 22,000 sequence variants per sample with a maximum count of 30,173 and a minimum count of 9,214. Samples were rarified to the minimum count used to establish relative abundance values of sequence variants commonly used in community level statistics and within the phyloseq R package (version 1.22.3) (17). Taxonomic identification of sequence variants was accomplished in Dada2 using a naive Bayesian classifier against a Dada2-formatted Silva 128 database (18). Differential abundances of sequence variants by culture status was performed using a negative binomial model through DeSeq2 (version 1.18.1) (19). Genus level counts of mycobacterium were split into two groups with equal membership using the discretize function of the Arules package (version 1.6-1). Visualizations in R were performed with ggplot2 (version 2.2.1) embedded within the phyloseq package. Microbiome data and the code to replicate the figures are freely available on Github at https://github.com/Strong-Lab/NTM_Soil.

Soil pH and mineralogy

Soil, saprolite, and fresh rock pH values were measured by adding de-ionized water to dried material (crushed in the case of fresh rock) until the pore space was saturated and the surface

glistened. A standard pH probe and meter were used and a unique calibration for each sample was generated by measuring pH 4, 7, and 10 buffer solutions.

Minerals were quantified by using a Rigaku MiniFlex 600 X-ray diffractometer (XRD) employing copper radiation and a scintillation detector with a graphite monochromator as a practical, rapid screening and characterization tool for complex soil mixtures. Mineral abundances were quantified by standard Rietveld methods embedded in the Rigaku PDXL2 software. Following filtering of columns with sparse information, the resulting matrix contained 11 features for examination including: magnetite, hematite, ilmenite, maghemite, gibbsite, carbonate minerals, quartz, pH, plagioclase, 1:1 clays, and goethite **(Table 1).**

Feature Correlation Analyses

Feature correlation analyses were used to identify and determine the strength of correlation between features and response variables. Soil mineralogy was populated using 55 soil samples. The response variable tested was NTM culture status (culture positive or culture negative). Soil characteristics and culture status were imported into a Pandas (version 0.20.3) Dataframe object in a Jupyter Notebook (version 4.3.0) using Python (version 3.6). The StandardScaler function from the Scikit-learn package (version 0.19.1) was used to normalize soil characteristic percentages within each feature column. The Shapiro-Wilks function from the Scipy package (version 1.0.0) was used to test the normality of each column in both culture status groups. If either group rejected the null hypothesis, a non-parametric Wilcoxon signed-rank test was used to test for significance between NTM culture status. Otherwise, a t-test with unequal variances was employed to test between the 2 distributions. Feature importance was calculated with the

permutation importance function within eli5 (version 0.8.2). Feature values were shuffled in 1000 permutations creating an effect of removing the information from a given feature on the performance of a classifier. Thus, features were assigned a mean decrease in accuracy (MDA) signifying how important a feature was to the accuracy of a machine learning model (**Supplementary Figure 1)**. MDA features scores were represented in decimal format using Seaborn (version 0.9.0). The balance of samples in our model and the unexplained variance of NTM culture status, limits the performance of a classification model and thus, the overall values of the feature scores (20). The relationship of MDA scores was used to select important features for downstream *in vitro* growth assays. Feature scores changed slightly in each iteration. However, the ordering of importance and significance of the relationships between features remained intact. MDA scores and standard deviations were averaged into a group designated as "all remaining features" when not the focus of the soil composition analysis. Feature importance scores only identified soil characteristics useful for accuracy of a machine learning classifier, however, feature importance did not indicate a significant correlation between the abundance of soil features and the outcome variable.

***In vitro* NTM growth assays in the presence of soil components and sterilized soil samples.**

General information for the individual minerals tested in this study are included in **Table 1.** The HNL 12-48 soil sample was identified to be rich in kaolinite and free of halloysite and gibbsite. The RAP samples were recovered, by rappelling, from a sea cliff on the northern shoreline of the Kohala Peninsula of the Big Island (21). These samples were selected due to the presence of significant quantities of gibbsite and halloysite. Synthetic gibbsite was provided by Barry Bickmore, Ph.D., Brigham Young University (BYU) Research Collections. Pure birnessite

196 was synthesized by acid titration (22). Crushed hematite was obtained from the BYU research
197 mineral collection. Kaolinite (#K1512) and halloysite (#685445) were obtained from Sigma
198 Aldrich and maghemite was obtained from U.S. Research Nanomaterials, #1309-37-1. After
199 completing a mineral dose response assay for *M. abscessus* **(Supplementary Figure 2)** and *M.*
200 *chimaera* **(Supplementary Figure 3),** 100 mg/ml of mineral was chosen for *in vitro* growth
201 experiments. Soil samples were autoclaved at 132 °C for 15 minutes, plated on standard
202 Middlebrook 7H10 mycobacterial culture agar (24), and incubated at 37 °C for a minimum of
203 three days to ensure sample sterility. All particles were suspended to 100 mg/mL in standard
204 mycobacterial culture broth media Middlebrook 7H9 (25) supplemented with 10% albumin-
205 dextrose-catalase (ADC), 2 % glycerol and 0.05 % Tween 80. These reagents, both autoclaved
206 and non-sterile, were also characterized with the Rigaku Miniflex using their CapWow capillary
207 spinner sample holder. Small samples are loaded into 1 mm Kapton tubes and are rotated in the
208 X-ray beam, effectively creating a random orientation during analysis.
209
210 One mL of all suspensions in low bind microcentrifuge tubes were inoculated with 1 x 10^5
211 CFU/mL of 12-45-Sw-A-1 *M. abscessus* or 5 x 10^5 CFU/mL of 12-56-S-1-1 *M. chimaera* or *M.*
212 *avium* H87 and incubated on a rotating stand at 37 °C (26, 27). The same concentrations of NTM
213 were added to 1 ml 7H9 broth as untreated controls. At the 1, 24, 48 and 96-hour timepoints post
214 inoculation, the cultures were serially diluted in 7H9 broth, and the dilutions were plated in
215 duplicate onto 7H10 agar supplemented with 10 % ADC and incubated at 37 °C. To determine
216 changes in colony forming units (CFU), the plates were counted three days post incubation for
217 *M. abscessus* and 10-14 days post incubation for *M. chimaera* and *M. avium.*
218

Scanning Electron Microscopy (SEM)

SEM images were obtained for *M. abscessus* and *M. chimaera* grown for 48 hours in the presence of hematite, gibbsite, birnessite, and untreated controls. Suspensions were filtered through a 0.2 micron Isopore™ (#R8MA21491) membrane filter. Next, the samples were fixed with 3 % glutaraldehyde in 0.1 M cacodylate buffer (pH 7.3) for 16 hours, rinsed with distilled water three times for ten minutes, treated with 1 % OsO_4 at 4 °C for 16 hours, and rinsed again with distilled water. Samples were dehydrated by rinsing for ten minutes with ethanol at concentrations of 30, 50, 70, 80, 90, 96 and 100 % at 25 °C, followed by acetone rinses at 30, 50 and 100 % concentrations. Samples were then dried with a critical point dryer, mounted on aluminum SEM stubs with double-sided carbon tape, and coated with a gold-palladium alloy. A FEI Apreo scanning electron microscope at BYU obtained six megapixel secondary-electron images in a low vacuum with a 10 kV and 0.1 nA beam.

***In vitro* data analysis**

Differences in log10 CFU/mL between NTM cultures exposed to clays/minerals and unexposed/control cultures were estimated using ANOVA models with robust sandwich covariance estimators. Separate models were run for each NTM species (*M. abscessus*, *M. chimaera*, and *M. avium*) at each post-exposure time point (1hr, 48hr, 96hr, and, in some experiments, 24hr). Comparisons were made between clay soils, between synthetic clays, between iron-bearing minerals, and between manganese-bearing minerals. ANOVA analyses were performed in R (28) version 3.6.3. Robust covariance estimation was performed using the sandwich package (29) version 2.5-1.

RESULTS

Less diverse microbiome in NTM-culture positive soil samples

Of the total soil samples from this study, a subset (n=18, eight NTM culture positive and ten NTM culture negative) were subjected to exploratory microbiome analyses. Linear modeling of mycobacterium genus counts against pH and culture status revealed no significant relationships ($F = 1.007$, $p = 0.330$ and $F = 1.119$, $p = 0.306$). Shannon diversity index was used to compare species richness between NTM culture positive and NTM culture negative groups. The Shannon diversity values between NTM culture groups showed a trend towards significance with NTM culture positive samples having a lower overall diversity compared to NTM culture negative samples **(Supplementary Figure 4A).** Taxonomic analysis revealed the phylum *Firmicutes* was significantly enriched in NTM culture positive samples **(Supplementary Figure 4B)** and the phylum composition varied by culture status **(Supplementary Figure 4C).** Similar trends in Shannon diversity and overall Phyla abundance were also observed when the data were stratified by mycobacteria genus counts **(Supplementary Figure 5A-B).**

NTM recovery is not driven by soil pH

Soil were subjected to pH analyses. Overall, there was a statistically significant difference in soil pH among the individual islands. Specifically, of the five islands examined, pH of Hawai'i Island soil was more acidic (mean, pH = 5.4) compared to the soil pH = 7.1-7.6 of the other four islands **(Figure 2A).** However, pH did not significantly vary when the data was stratified by NTM culture results **(Figure 2B)**. Compared to an average of all other features in the dataset, the importance of pH as a feature had a lower mean decrease in accuracy **(Figure 2C).**

Gibbsite, a clay mineral, inhibits both *M. abscessus* and *M. chimaera in vitro*

Exploratory feature importance selection was then performed against the full dataset to elucidate possible clay characteristics that correlate to the presence of NTM. Based on our feature prediction models, gibbsite (a clay mineral) and 1:1 clays (a group of structurally related minerals where the fundamental building block consists of a sheet of silicate tetrahedra bonded to a layer of Al-O-OH or Mg-O-OH octahedra which includes kaolinite and halloysite, the most common 1:1 clays in Hawai'i) (30, 31) were predicted to be less important compared to all other features in the dataset **(Figure 3A).** Alternatively, based again on our machine learning models, NTM culture negative samples were predicted to have more gibbsite and 1:1 clays when stratified by culture status **(Supplementary Figure 6A)**. To directly test these hypotheses, gibbsite and the clays, kaolin and halloysite, were incubated separately in the presence of NTM. Synthetic gibbsite significantly inhibited the growth of both *M. abscessus* and *M. chimaera in vitro* **(Figure 3B-C)** as well as *M. avium* at 48 hours **(Supplementary Figure 7A)** compared to the untreated controls. The growth of *M. abscessus* and *M. chimaera* were not significantly altered by exposure to kaolin or halloysite **(Figure 3B-C)**, but halloysite significantly facilitated the growth of *M. avium* at 96 hours **(Supplementary Figure 7A).**

To investigate whether the aforementioned results could be replicated using actual soil samples, three Hawai'i soil samples were identified to contain: 1) 100 % kaolinite (HNL 12-48), 2) 35 % halloysite/27 % gibbsite (RAP2-2), or 3) 55 % halloysite (RAP2-5). Similar to Figure 3B, the growth of *M. abscessus* was not impacted when co-cultured with HNL 12-48, a soil comprised of 100 % kaolinite **(Figure 3D)**; in contrast, significantly less *M. chimaera* was recovered **(Figure**

3E). The inhibitory effect of gibbsite on NTM growth was lost when incubated with soil containing both gibbsite and halloysite (Figure 3D-E). *M. abscessus* showed significantly higher growth early after exposure to RAP2-5 (1 and 48 hours) and RAP2-2 soil samples (48 hours); however, incubation with these soils did not affect *M. chimaera* growth *in vitro* compared to the bacteria alone group (untreated) **(Figure 3D-E)**.

Iron minerals significantly increase NTM growth *in vitro*

Based on our feature prediction modeling, iron oxide minerals such as maghemite, hematite, and magnetite are posited to be of greater importance than the combination of all remaining features **(Figure 4A)**. To estimate the directionality of maghemite, hematite, and magnetite to NTM growth, the amount of these iron oxides in each soil sample were plotted against NTM culture status, predicting more hematite and maghemite in NTM-positive cultures **(Supplementary Figure 6B).** Tested *in vitro*, the growth of *M. abscessus* was generally significantly enhanced in the presence of hematite and maghemite compared to the untreated control **(Figure 4B)**. While greater counts of *M. chimaera* were observed for all iron oxides tested at the 24-hour mark compared to the untreated control **(Figure 4C),** growth decreased at the 48-hour timepoint in the samples incubated with maghemite and magnetite **(Figure 4C).** However, CFU abundance in the samples was equivalent by the 96 hour timepoint for all M. *chimaera* samples. Similar to *M. abscessus*, significantly more *M. avium* was observed when incubated with hematite **(Supplementary Figure 7B).**

Manganese minerals show varied affects on NTM growth *in vitro*

309 Because soil manganese has been associated with lower risk for NTM infections (7, 9), the
310 effects of manganese minerals on NTM growth was tested. *M. abscessus*, *M. chimaera*, and *M.*
311 *avium* were incubated in the presence of manganese minerals including synthetic pyrolusite,
312 manganite, cryptomelane, or birnessite. Results were varied. In general, the growth of all NTM
313 tested was significantly higher when cultured in the presence of the manganese oxide pyrolusite
314 **(Figure 5A-B, Supplementary Figure 7C).** While the growth of *M. abscessus* was also higher
315 in the presence of cryptomelane (24 and 48 hours), *M. chimaera* growth was significantly
316 inhibited by the 96 hour timepoint. Less *M. chimaera* was also observed in the presence of the
317 manganese oxide mineral, birnessite. Of importance, birnessite also significantly inhibited the
318 growth of *M. avium* (**Supplementary Figure 7C**), while showing little affect on *M. abscessus*
319 viability.
320
321 **Pictorial of NTM attachment to mineral surfaces**
322 *In vitro* assays demonstrated more numbers of *M. abscessus* and *M. chimaera* in the presence of
323 hematite, whereas gibbsite and birnessite significantly inhibited the growth of NTM. Scanning
324 electron microscope images show *M. abscessus* (**Figure 6A)** and *M. chimaera* **(Figure 6B)** alone
325 and in association with hematite **(Figure 6E-F),** whereas no bacilli are seen in the presence of
326 gibbsite **(Figure 6C-D)** and birnessite (**Figure 6G-H)**.

DISCUSSION

Infections due to NTM are a growing clinical concern across the U.S. and many parts of the world due to their increasing prevalence and their recalcitrant nature to current chemotherapeutic treatments. It is widely recognized that environmental exposures contribute to NTM acquisition. While not as widely sampled or well-characterized as water-associated biofilms, NTM occupy soil niches globally. Because 80-90 % of microbes in soil are attached to solid surfaces, understanding the specific components of soil that contribute to NTM growth and maintenance in a geographic focal point for infection like Hawai'i is imperative (32). In this study, we performed microbiome, mineralogic studies, and applied permuted feature importance approaches to predict soil components associated with NTM. We then tested the ability of these soil components to directly modulate the growth of native NTM isolates from Hawai'i *in vitro* and used high-powered microscopy to capture the capability of NTM to bind to these components.

The microbiome study demonstrated a trend towards lower alpha diversity in the NTM culture positive samples suggesting reduced richness of species compared to the NTM culture negative samples (Supplementary Figure 4A). If the trend of lower alpha diversity in NTM culture positive samples remains true when the sample size increases, this metric could potentially become a useful feature to predict NTM presence or absence in soil. Alpha diversity may also be linked to the soil composition and competition for resources.

A variety of soil factors, or a combination of factors, could contribute to the presence or absence of environmental NTM. When analyzed as a single factor, soil pH was not found to be a significant driver for NTM diversity in this study (Figure 2B), despite NTM showing a preference for acidic environmental conditions (pH 3-5) (*e.g.*, acidic, brown water swamps, fulvic and humic acids, and peat-rich potting soils) (33-35). Most soils in Hawai'i have pH ranges from 4-8, but most are acidic due to the warm temperatures and high rainfall, leading to elevated pCO_2 values in the atmosphere. However, a primary driver of low pH in deeply weathered soils is the lack of base cations. Because we observed Hawai'i Island soil as more acidic compared to the other islands examined, future studies should further elucidate the role of soil pH to NTM growth.

A primary aim of this work was to determine important soil mineralogical features associated with NTM culture status by using machine learning tools to identify important features then validating the impact of these minerals on NTM growth *in vitro*. Overall, soil feature distributions did not correlate directly with *in vitro* NTM culture assays. This may be a result of the limited power and the unbalanced outcome groupings. Yet, by using feature importance measures, we were able to identify gibbsite as possible modulator of NTM growth (Figure 3A) and confirmed that alone, pure gibbsite significantly inhibits the growth of *M. abscessus* and *M. chimaera* (Figure 3B-C). Gibbsite is one of the mineral forms of aluminum hydroxide that forms the weathered surfaces of clays. Prior work detailing the soil composition of the Colombian Amazon has shown aluminum in clay possess antibacterial activity against other microorganisms, including *Escherichia coli* (36). While gibbsite is common in tropical soils (37), the amount of gibbsite or its interaction with other minerals may influence the presence or

absence of NTM in Hawai'i soil. Beyond the examination of aluminum as a single factor, the combination of aluminum and iron has been shown to increase the production of reactive oxygen species in prokaryotes, which can cause cell death (38). Noteworthy of discussion, the inhibitory effect of gibbsite on NTM growth was lost when incubated with soil containing gibbsite and halloysite (Figure 3D-E). It's possible that the surface chemistry and crystal size of pure gibbsite change when in a complex mixture such as soil containing other minerals (*e.g.*, halloysite). Similar discrepancies were also observed for *M. chimaera* incubated with pure kaolin or kaolinite-containing soil. Incubation of *M. chimaera* with pure kaolin did not alter CFU counts at the timepoints tested (Figure 3C); however, significantly less *M. chimaera* was recovered overtime when incubated in soil containing kaolinite (Figure 3E). Besides kaolinite, it's possible the soil sample also contained other unidentified minerals or other factors that inhibited *M. chimaera* growth. It would be prudent to perform more detailed chemical analyses of these particular soils in the future.

The presence of iron in soil can promote NTM growth and our feature predictions posit this is also true in Hawai'i soil (Figure 4A). Our *in vitro* data indicate that not all iron oxide minerals such as maghemite, magnetite, and hematite impact the growth of NTM equally. For example, *M. abscessus* growth was facilitated in the presence of all iron oxides tested, particularly hematite (Figure 4B), which was also associated with higher growth of *M. avium* (Supplementary Figure 7B), but little impact on *M. chimaera* (Figure 4C). Hematite has already been shown to promote the growth of soil-dwelling *Pseudomonas mendocina* by acting as an iron source *in vitro* (39). Because of the importance of iron-sequestration by NTM, it would be prudent for future work to dissect the role of *M. abscessus*, *M. chimaera*, and *M. avium*

siderophores on iron sequestration from soil. Additionally, the impact of iron oxides on NTM biofilm development is an avenue for future study given the known effect of iron on the growth of *M. smegmatis* and *M. tuberculosis* biofilms (40, 41).

Manganese is an important minor element commonly found in basalts and other mafic rocks and is implicated as an inhibitory agent for NTM in soil. Although numerous manganese oxides and hydroxides (*e.g.*, pyrolusite, manganite, and cryptomelane) have been identified, birnessite is one of the most common in soil (42). Birnessite demonstrated potent antibacterial activity against both SGM *M. chimaera* (Figure 5B) and *M. avium* (Supplementary Figure 7C), but did not affect the growth of RGM *M. abscessus* (Figure 5A). *M. chimaera* growth was impaired in the presence of cryptomelane by the 96 hour timepoint. Interestingly, the manganese oxide, pyrolusite facilitated the growth of all three NTM species tested. In other studies, manganese oxide nanoparticles were found to exert antibacterial activity against *Vibrio cholerae*, *Shigella*, and *E. coli* and birnessite has been shown to inhibit pathogenic prions (43, 44). The role of manganese oxides/hydroxides in NTM growth in Hawaiian soils remains an open question. Additional work would be required to identify how manganese negatively or positively impacts NTM growth in the environment.

SEM images augment the culturing studies by illustrating the relationships between mineral substrates and NTM cells, although fixation and rinsing steps in mount preparations may not preserve a 1:1 relationship between cells and cell attachment versus abundances in culturing experiments. *M. abscessus* was seen in abundance attached to the surfaces of hematite grains and on the filter membrane of the mineral-free control culture, whereas it was not observed in the

418 presence of birnessite and gibbsite (Figure 6). Similar relationships were observed for *M.*
419 *chimaera*. This species was found in the presence of hematite, although not in the relatively high
420 proportions exhibited by *M. abscessus*, but was absent on gibbsite or birnessite (Figure 6).
421 The absence of NTM in the presence of pure gibbsite (Figure 3B-C) may be due to aluminum
422 toxicity (36). In addition, gibbsite is very fine grained, with crystallites < 1 µm in diameter
423 (Figure 6), which may preclude attachment to a single grain. Similarly, individual birnessite
424 grains are very small and unfavorable for attachment. Presumably some aspect of the surface
425 chemistry of birnessite may also contribute to the inhibition of *M. chimaera* and *M. avium* in
426 soil.
427
428 This study introduced the possibility that transition metals and oxide features in soil influence
429 NTM growth *in vitro*. Future work should elucidate the various mechanisms used by NTM to
430 evade toxicity of soil factors to promote extended survival in the environment. For example,
431 RGM including *M. fortuitum* and *M. chelonae* have been shown to resist exposure to transitional
432 metals such as mercury through actions of protective mercuric reductases and organomercurial
433 lyases (45, 46). In addition, the type VII secretion systems (*e.g.*, ESX-3) of environmental
434 mycobacteria have been associated with iron acquisition via mycobactin, a secreted iron chelator
435 that promotes survival (47). Finally, it's possible NTM also utilize other siderophores, chelating
436 proteins such as calprotectins, or structures similar to "zincosomes" (zinc-holding compartments)
437 produced by *Mycobacterium tuberculosis*, as multi-faceted mechanisms to protect from soil
438 toxicity including control of uptake, oxidation, sequestration inside the bacteria, and efflux of
439 toxic soil materials (48).
440

This study has some limitations. Soil samples were unequally collected from a limited number of sites across Oahu, Kauai, Hawai'i Island, Molokai, and Maui (Figure 1). Collecting an increased number of soils that more widely and equally represent the different geographic areas across the islands would not only increase the limited sample size, but will also provide a more complete study set to more robustly identify features influencing NTM growth. Increasing the number of NTM culture positive samples with defined soil characteristics would also improve the balance of the dataset and the overall feature selection performance. The addition of more samples would also increase the power of comparisons in the microbiome analysis. A single concentration of each mineral was used to compare across species and timepoints; however, the growth of NTM may be modulated with lower or higher amounts of compounds. Because soil is a complex mixture of many different components, we also cannot rule out the role of all other soil components (*e.g.*, sodium, zinc, copper, organic material) or other environmental factors such as rainfall and humidity in NTM growth and sustainability. Finally, because we were interested in studying *M. abscessus* and *M. chimaera*, clinically relevant NTM found in the lung, these experiments were performed at 37 °C; however soil temperature likely varies widely in the environment and these results might change with lower incubation temperature.

In closing, this study is the first to our knowledge to characterize the soil composition in detail and relate that to NTM culture status. This study also identified important minerology features in Hawai'i soil using the application of machine learning tools which were then validated *in vitro*. In addition, this study captured microscopy images of NTM binding to soil features. Because gibbsite and some of the manganese oxides were shown to decrease NTM growth and hematite and pyrolusite promoted growth, it would be prudent to quantify these components and others in

464 other soil samples globally in future work with subsequent translation of these findings to the
465 presence or absence of clinically relevant NTM species in the environment.

466 **ACKNOWLEDGEMENTS**

467 The authors would like to thank Joseph O. Falkinham, III Ph.D. and Myra Williams for their
468 early assistance with NTM culture. This work was funded, in part, by the National Science
469 Foundation Grant #1743587 Division of Environmental Biology, as part of the Evolution of
470 Infectious Diseases Program. JRH also acknowledges support from the Padosi Foundation. The
471 funders had no role in the study design, data collection and interpretation, or the decision to
472 submit the work for publication.

473 **FIGURE LEGENDS**

474

475 **Figure 1. Hawai'i soil map**. **A)** Location of soil samples in the Hawaiian Islands, with NTM
476 positive (green stars) and NTM negative soils (black dots) as indicated. **B)** Map of Oahu
477 indicating NTM positive and negative soils. Blue contours are mean annual rainfall (mm/yr).
478 Red indicates the presence of bedrock at the surface and the other map colors represent various
479 soil orders (USDA, 2019).

480

481 **Figure 2. NTM culture results are not related to soil pH. A)** pH was measured from soil
482 samples collected from Oahu (n = 46), Hawai'i Island (n = 4), Molokai (n = 4), Kauai (n = 5),
483 and Maui (n = 1). pH value distributions were plotted by island and tested for differences (One-
484 way ANOVA, *, p = 0.01). **B)** Soil samples were stratified by NTM culture status and all pH
485 values are plotted. NTM culture negative samples, pH mean = 6.95 (n = 49); NTM culture
486 positive samples, pH mean = 6.89 (n = 11) (One-way ANOVA, NS, p = 0.85). **C)** Feature
487 importance is defined by mean decrease in accuracy (MDA) after 1.000 iterations of a classifier
488 while shuffling the feature values. A higher MDA is associated with an important feature in the
489 model. All remaining features is an average of the importance and variation amongst features
490 other than pH. The importance of pH is lower than the average of all remaining features (0.0197
491 ± 0.0145 vs 0.0367 ± 0.0128, ***, $p < 0.0001$).

492

493 **Figure 3. Impact of clay minerals on the *in vitro* growth of native Hawai'i environmental**
494 **NTM isolates. A)** Distribution of clay mineral mean decrease in accuracy across 1,000 iterations
495 of shuffling. The importance of gibbsite is less than the average of the remaining features

(0.0302 ± 0.0117 vs 0.0377 ± 0.0141). However, the importance of gibbsite is greater than 1:1 clay (0.0302 ± 0.0117 vs 0.0172 ± 0.0041). **B)** *In vitro* growth of *M. abscessus* in the presence of synthetic gibbsite, kaolin and halloysite. **C)** *In vitro* growth of *M. chimera* in the presence of synthetic gibbsite, kaolin, or halloysite. **D)** *In vitro* growth of *M. abscessus* in the presence of Hawai'i soil. **E)** *In vitro* growth of *M. chimaera* in the presence of Hawai'i soil. *** $p < 0.001$, **** $p < 0.0001$.

Figure 4. Impact of iron minerals on the *in vitro* growth of native Hawai'i environmental NTM isolates. A) Distribution of iron oxide mean decrease in accuracy across 1,000 iterations of shuffling. The lowest iron oxide mineral (maghemite) is greater than the average of all remaining features suggesting iron oxide minerals are important for NTM growth (0.0569 ± 0.0160 vs 0.0196 ± 0.0092). Magnetite is of greater importance than maghemite or hematite (0.0770 ± 0.0226 vs 0.0569 ± 0.0160 and 0.0581 ± 0.0185. **B)** *In vitro* growth of *M. abscessus* in the presence of synthetic maghemite, magnetite, and hematite. **C)** *In vitro* growth of *M. chimaera* in the presence of synthetic maghemite, magnetite, and hematite. * $p < 0.05$, ** $p < 0.01$, *** $p < 0.001$, **** $p < 0.0001$.

Figure 5. Impact of a manganese compound on the *in vitro* growth of native Hawai'i environmental NTM isolates. *In vitro* growth of *M. abscessus* **(A)** or *M. chimaera* **(B)** in the presence of synthetic manganese minerals. * $p < 0.05$, ** $p < 0.01$, *** $p < 0.001$, **** $p < 0.0001$.

518 **Figure 6. Scanning electron microscope images of environmental NTM isolates grown in**
519 **the presence of gibbsite, hematite, and birnessite. A-B)** *M. abscessus* (3 μm) and *M. chimaera*
520 (5 μm) in the absence of soil minerals. **C-D)** *M. abscessus* and *M. chimaera* in the presence of
521 gibbsite. **E-F)** *M. abscessus* and *M. chimaera* in the presence of hematite. **G-H)** *M. abscessus*
522 and *M. chimaera* in the presence of birnessite. Red arrows indicate the NTM bacilli.

References

1. Honda JR, Virdi R, Chan ED. 2018. Global Environmental Nontuberculous Mycobacteria and Their Contemporaneous Man-Made and Natural Niches. Front Microbiol 9:2029. doi: 10.3389/fmicb.2018.02029.
2. Walsh CM, Gebert MJ, Delgado-Baquerizo M, Maestre FT, Fierer N. 2019. A global survey of mycobacterial diversity in soil. Appl Environ Microbiol doi:10.1128/AEM.01180-19.
3. Lahiri A, Kneisel J, Kloster I, Kamal E, Lewin A. 2014. Abundance of Mycobacterium avium ssp. hominissuis in soil and dust in Germany - implications for the infection route. Lett Appl Microbiol 59:65-70. doi: 10.1111/lam.12243.
4. De Groote MA, Pace NR, Fulton K, Falkinham JO, 3rd. 2006. Relationships between Mycobacterium isolates from patients with pulmonary mycobacterial infection and potting soils. Appl Environ Microbiol 72:7602-6. doi; 10.1128/AEM.00930-06.
5. Fujita K, Ito Y, Hirai T, Kubo T, Maekawa K, Togashi K, Ichiyama S, Mishima M. 2014. Association between polyclonal and mixed mycobacterial Mycobacterium avium complex infection and environmental exposure. Ann Am Thorac Soc 11:45-53. doi: 10.1513/AnnalsATS.201309-297OC.
6. Fujita K, Ito Y, Hirai T, Maekawa K, Imai S, Tatsumi S, Niimi A, Iinuma Y, Ichiyama S, Mishima M. 2013. Genetic relatedness of Mycobacterium avium-intracellulare complex isolates from patients with pulmonary MAC disease and their residential soils. Clin Microbiol Infect 19:537-41. doi: 10.1111/j.1469-0691.2012.03929.x.
7. Adjemian J, Olivier KN, Seitz AE, Holland SM, Prevots DR. 2012. Prevalence of nontuberculous mycobacterial lung disease in U.S. Medicare beneficiaries. Am J Respir Crit Care Med 185:881-6. doi: 10.1164/rccm.201111-2016OC.
8. Honda JR, Hasan NA, Davidson RM, Williams MD, Epperson LE, Reynolds PR, Smith T, Iakhiaeva E, Bankowski MJ, Wallace RJ, Jr., Chan ED, Falkinham JO, 3rd, Strong M. 2016. Environmental Nontuberculous Mycobacteria in the Hawaiian Islands. PLoS Negl Trop Dis 10:e0005068. doi: 10.1371/journal.pntd.0005068.
9. Adjemian J, Olivier KN, Seitz AE, Falkinham JO, 3rd, Holland SM, Prevots DR. 2012. Spatial clusters of nontuberculous mycobacterial lung disease in the United States. Am J Respir Crit Care Med 186:553-8. doi: 10.1164/rccm.201205-0913OC.
10. Chou MP, Clements AC, Thomson RM. 2014. A spatial epidemiological analysis of nontuberculous mycobacterial infections in Queensland, Australia. BMC Infect Dis 14:279. doi: 10.1186/1471-2334-14-279.
11. Lipner EM, Knox D, French J, Rudman J, Strong M, Crooks JL. 2017. A Geospatial Epidemiologic Analysis of Nontuberculous Mycobacterial Infection: An Ecological Study in Colorado. Ann Am Thorac Soc 14:1523-1532. doi: 10.1513/AnnalsATS.201701-081OC.
12. Vitousek P. 2006. Ecosystem science and human-environment interactions in the Hawaiian archileago. J of Ecology 94:510-521. doi: 10.1111/j.1365-2745.2006.01119.x.
13. Zhao X, Epperson LE, Hasan NA, Honda JR, Chan ED, Strong M, Walter ND, Davidson RM. 2017. Complete Genome Sequence of Mycobacterium avium subsp. hominissuis Strain H87 Isolated from an Indoor Water Sample. Genome Announc 5. doi: 10.1128/genomeA.00189-17.

14. Epperson LE, Strong M. 2020. A scalable, efficient, and safe method to prepare high quality DNA from mycobacteria and other challenging cells. J Clin Tuberc Other Mycobact Dis 19:100150. doi: 10.1016/j.jctube.2020.100150.
15. Gilbert JA, Jansson JK, Knight R. 2014. The Earth Microbiome project: successes and aspirations. BMC Biol 12:69. doi: 10.1186/s12915-014-0069-1.
16. Callahan BJ, McMurdie PJ, Rosen MJ, Han AW, Johnson AJ, Holmes SP. 2016. DADA2: High-resolution sample inference from Illumina amplicon data. Nat Methods 13:581-3. doi: 10.1038/nmeth.3869.
17. McMurdie PJ, Holmes S. 2013. phyloseq: an R package for reproducible interactive analysis and graphics of microbiome census data. PLoS One 8:e61217. doi: 10.1371/journal.pone.0061217.
18. Quast C, Pruesse E, Yilmaz P, Gerken J, Schweer T, Yarza P, Peplies J, Glockner FO. 2013. The SILVA ribosomal RNA gene database project: improved data processing and web-based tools. Nucleic Acids Res 41:D590-6. doi: 10.1093/nar/gks1219.
19. Love MI, Huber W, Anders S. 2014. Moderated estimation of fold change and dispersion for RNA-seq data with DESeq2. Genome Biol 15:550. doi: 10.1186/s13059-014-0550-8.
20. Louppe G, Wehenkel, L., Sutera, A. and P. Geurts. 2013. Understanding variable importances in forests of randomized trees, on Neural Information Processing Systems Foundation, Inc. https://papers.nips.cc/paper/4928-understanding-variable-importances-in-forests-of-randomized-trees. Accessed
21. Sowards K, Nelson, S.T., McBride, J.H., Bickmore, B., Heizler, M.T., Tingey, D.G., Rey, K.A., and Yaede, J.R., . 2018 A Conceptual Model for the Rapid Weathering of Tropical Ocean Islands: A Synthesis of Geochemistry and Geophysics, Kohala Peninsula, Hawaii, USA. Geosphere, 14:1324-1342. doi: 10.1130/GES01642.1.
22. McKenzie RM. 1971. The synthesis of birnessite, cryptomelane, and some other oxides and hydroxides of manganese. Mineralogical magazine 38:493-502. doi: 10.1180/minmag.1971.038.296.12.
23. Haydel SE, Remenih CM, Williams LB. 2008. Broad-spectrum in vitro antibacterial activities of clay minerals against antibiotic-susceptible and antibiotic-resistant bacterial pathogens. J Antimicrob Chemother 61:353-61. doi: 10.1093/jac/dkm468.
24. Middlebrook G, Cohn ML. 1958. Bacteriology of tuberculosis: laboratory methods. Am J Public Health Nations Health 48:844-53. doi: 10.2105/ajph.48.7.844.
25. Dubos RJ, Middlebrook G. 1947. Media for tubercle bacilli. Am Rev Tuberc 56:334-45.
26. Malcolm KC, Caceres SM, Honda JR, Davidson RM, Epperson LE, Strong M, Chan ED, Nick JA. 2017. Mycobacterium abscessus Displays Fitness for Fomite Transmission. Appl Environ Microbiol 83. doi: 10.1128/AEM.00562-17.
27. Kim E, Kinney WH, Ovrutsky AR, Vo D, Bai X, Honda JR, Marx G, Peck E, Lindberg L, Falkinham JO, 3rd, May RM, Chan ED. 2014. A surface with a biomimetic micropattern reduces colonization of Mycobacterium abscessus. FEMS Microbiol Lett doi:10.1111/1574-6968.12587. doi: 10.1111/1574-6968.12587.
28. Team RC. 2020 R: A language and environment for statistical computing. R Foundation for Statistical Computing. https://www.R-project.org/. Accessed
29. A Z. 2004. Econometric Computing with HC and HAC Covariance Matrix Estimators. Journal of Statistical Software 11:1-17.
30. Barton CD, Karathanasis AD. 2002. Clay Minerals, p In (ed), Encyclopedia of Soil Science, ed vol

31. Nelson ST, Tingey DG, Selck B. 2013. The denudation of ocean islands by ground and surface waters: The effects of climate, soil thickness, and water contact times on Oahu, Hawaii Geochimica et Cosmochimica 103:276-294. doi: 10.1016/j.gca.2012.09.046.
32. Renella PNJAMTCLLGPG. 2003. Microbial diversity and soil functions. European Journal of Soil Science 54:655-670. doi: 10.1111/ejss.4_12398.
33. Kirschner RA, Jr., Parker BC, Falkinham JO, 3rd. 1992. Epidemiology of infection by nontuberculous mycobacteria. Mycobacterium avium, Mycobacterium intracellulare, and Mycobacterium scrofulaceum in acid, brown-water swamps of the southeastern United States and their association with environmental variables. Am Rev Respir Dis 145:271-5. doi: 10.1164/ajrccm/145.2_Pt_1.271.
34. Portaels F, Pattyn SR. 1982. Growth of mycobacteria in relation to the pH of the medium. Ann Microbiol (Paris) 133:213-21.
35. Bodmer T, Miltner E, Bermudez LE. 2000. Mycobacterium avium resists exposure to the acidic conditions of the stomach. FEMS Microbiol Lett 182:45-9. doi: 10.1111/j.1574-6968.2000.tb08871.x.
36. Londono SC, Hartnett HE, Williams LB. 2017. Antibacterial Activity of Aluminum in Clay from the Colombian Amazon. Environ Sci Technol 51:2401-2408. doi: 10.1021/acs.est.6b04670.
37. Galán E. 2006. Genesis of clay minerals. . Developments in Clay Science 1:1129-1162. doi: 10.1016/S1572-4352(05)01042-1.
38. Exley C, Mold MJ. 2015. The binding, transport and fate of aluminium in biological cells. J Trace Elem Med Biol 30:90-5. doi: 10.1016/j.jtemb.2014.11.002.
39. Hersman LE, Forsythe JH, Ticknor LO, Maurice PA. 2001. Growth of Pseudomonas mendocina on Fe(III) (hydr)oxides. Appl Environ Microbiol 67:4448-53. doi: 10.1128/AEM.67.10.4448-4453.2001.
40. Ojha A, Hatfull GF. 2007. The role of iron in Mycobacterium smegmatis biofilm formation: the exochelin siderophore is essential in limiting iron conditions for biofilm formation but not for planktonic growth. Mol Microbiol 66:468-83. doi: 10.1111/j.1365-2958.2007.05935.x.
41. Ojha AK, Baughn AD, Sambandan D, Hsu T, Trivelli X, Guerardel Y, Alahari A, Kremer L, Jacobs WR, Jr., Hatfull GF. 2008. Growth of Mycobacterium tuberculosis biofilms containing free mycolic acids and harbouring drug-tolerant bacteria. Mol Microbiol 69:164-74. doi: 10.1111/j.1365-2958.2008.06274.x.
42. Gilkes RJ, & McKenzie, R. M. . 1988. Geochemistry and mineralogy of manganese in soils. In Manganese in soils and plants. Springer, Dordrecht:22-35. doi: 10.1007/978-94-009-2817-6_3.
43. Chowdhury AN, Azam MS, Aktaruzzaman M, Rahim A. 2009. Oxidative and antibacterial activity of Mn3O4. J Hazard Mater 172:1229-35. doi: 10.1016/j.jhazmat.2009.07.129.
44. Russo F, Johnson CJ, Johnson CJ, McKenzie D, Aiken JM, Pedersen JA. 2009. Pathogenic prion protein is degraded by a manganese oxide mineral found in soils. J Gen Virol 90:275-80. doi: 10.1099/vir.0.003251-0.
45. Steingrube VA, Wallace RJ, Jr., Steele LC, Pang YJ. 1991. Mercuric reductase activity and evidence of broad-spectrum mercury resistance among clinical isolates of rapidly growing mycobacteria. Antimicrob Agents Chemother 35:819-23. doi: 10.1128/aac.35.5.819.

660 46. Steingrube VA, Murphy D, McMahon S, Chapman JS, Nash DR. 1975. The effect of
661 metal ions on the atypical mycobacteria: growth and colony coloration. Zentralbl
662 Bakteriol Orig A 230:223-36.
663 47. Siegrist MS, Unnikrishnan M, McConnell MJ, Borowsky M, Cheng TY, Siddiqi N,
664 Fortune SM, Moody DB, Rubin EJ. 2009. Mycobacterial Esx-3 is required for
665 mycobactin-mediated iron acquisition. Proc Natl Acad Sci U S A 106:18792-7. doi:
666 10.1073/pnas.0900589106.
667 48. Neyrolles O, Wolschendorf F, Mitra A, Niederweis M. 2015. Mycobacteria, metals, and
668 the macrophage. Immunol Rev 264:249-63. doi: 10.1111/imr.12265.
669

670 **Table 1:** Information about the minerals used in this study

Mineral:	**Mineral Group:**	**Formula:**	**Experiment:**
1:1 Clays	1:1 Clays	$Al_2Si_2O_5(OH)_4$	*in silico*
Halloysite	1:1 Clay (natural)	$Al_2Si_2O_5(OH)_4$	*in vitro*
Kaolinite	1:1 Clay (natural)	$Al_2Si_2O_5(OH)_4$	*in vitro*
Gibbsite	Clay (synthetic)	$Al(OH)_3$	Both
Magnetite	Fe-Ti-oxide/hydroxide	Fe_3O_4	Both
Maghemite	Fe-Ti-oxide/hydroxide	Fe_2O_3	Both
Hematite	Fe-Ti-oxide/hydroxide	Fe_2O_3	Both
Ilmenite	Fe-Ti-oxide/hydroxide	$FeTiO_3$	*in silico*
Goetithe	Fe-Ti-oxide/hydroxide	$FeO(OH)$	*in silico*
Calcite/Aragonite	Carbonate minerals	$CaCO_3$	*in silico*
Plagioclase	Feldspar	$NaAlSi_3O_8$ | $CaAl_2Si_2O_8$	*In silico*
Pyrolusite	Mn-oxide (natural)	MnO_2	*in vitro*
Cryptomelane	K-, Mn-oxide (natural)	$K(Mn)_8O_{16}$	*in vitro*
Birnessite	K-, Mn-oxide (synthetic)	$K(Mn)_2O_4 \cdot 1.5H_2O$	*in vitro*
Manganite	Mn-oxide/hydroxide (natural)	$MnO(OH)$	*in vitro*

671

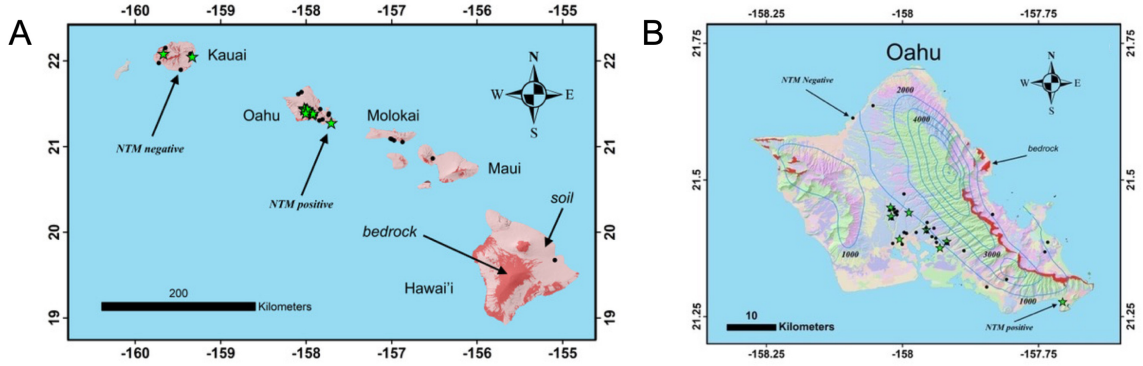

Figure 1. Hawai'i soil map. **A)** Location of soil samples in the Hawaiian Islands, with NTM positive (green stars) and NTM negative soils (black dots) as indicated. **B)** Map of Oahu indicating NTM positive and negative soils. Blue contours are mean annual rainfall (mm/yr). Red indicates the presence of bedrock at the surface and the other map colors represent various soil orders (USDA, 2019; https://www.nrcs.usda.gov/wps/portal/nrcs/detail/soils/edu/?cid=nrcs142p2_053588).

Figure 1
Glickman and Virdi, *et al*

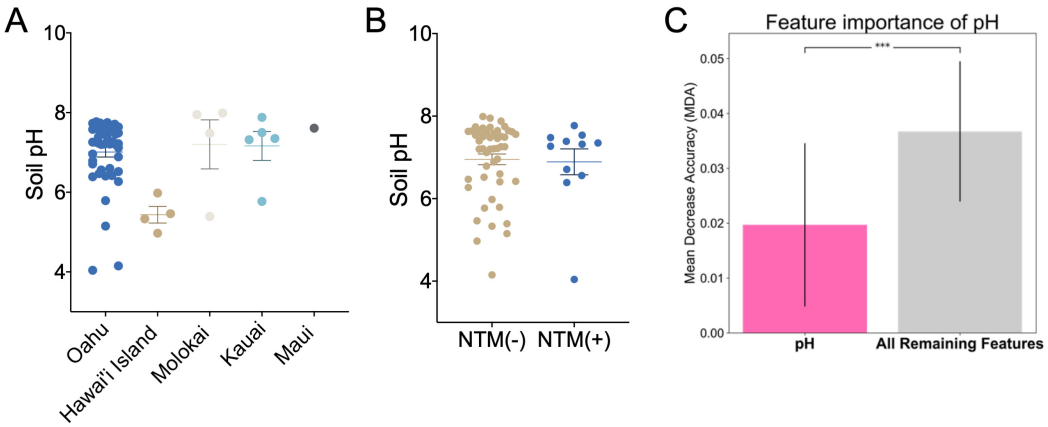

Figure 2. NTM culture results are not related to soil pH. A) pH was measured from soil samples collected from Oahu (n=46), Hawai'i Island (n=4), Molokai (n=4), Kauai (n=5), and Maui (n=1). pH value distributions were plotted by island and tested for differences (one-way ANOVA, *, $p = 0.01$). **B)** Soil samples were stratified by NTM culture status and all pH values plotted. NTM culture negative samples, pH mean = 6.95 (n=49); NTM culture positive samples, pH mean = 6.89 (n=11) (one-way ANOVA, NS, $p = 0.85$). **C)** Feature importance is defined by mean decrease in accuracy (MDA) after 1,000 iterations of a classifier while shuffling the feature values. A higher MDA is associated with an important feature in the model. All remaining features are an average of the importance and variation among features other than pH. The importance of pH is lower than the average of all remaining features (0.0197 ± 0.0145 vs 0.0367 ± 0.0128, ***, $p < 0.0001$).

Figure 2
Glickman and Virdi, *et al*

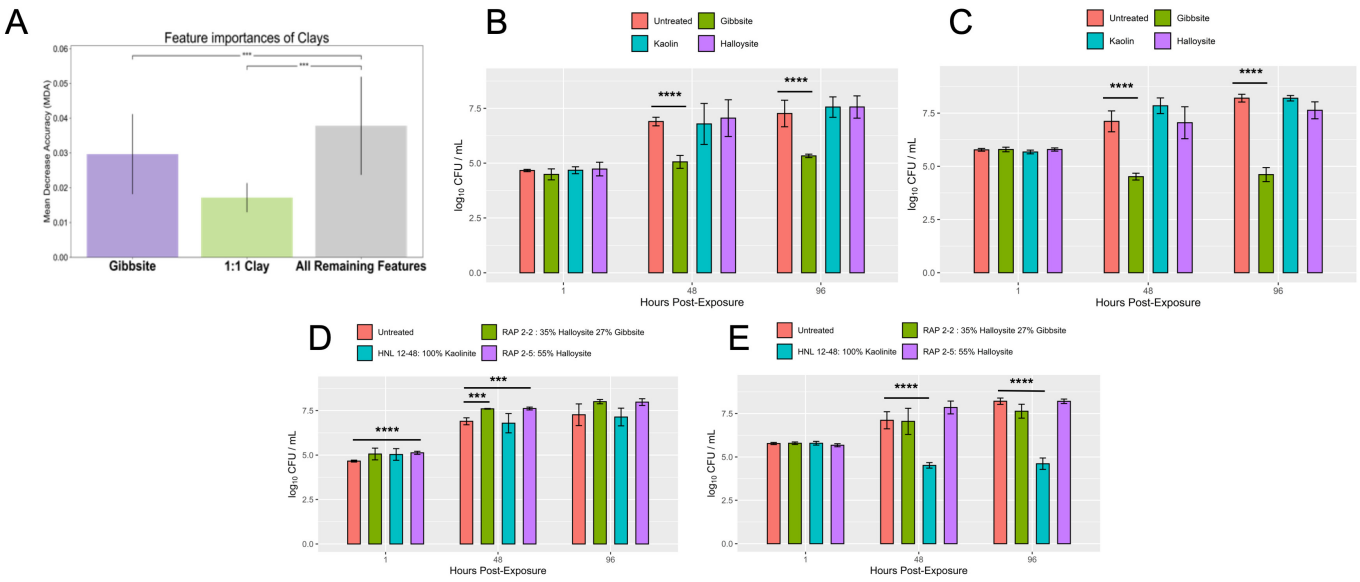

Figure 3. Impact of clay minerals on the *in vitro* growth of native Hawai'i environmental NTM isolates. A) Distribution of clay mineral mean decrease in accuracy across 1,000 iterations of shuffling. The importance of gibbsite is less than the average of the remaining features (0.0302 ± 0.0117 vs 0.0377 ± 0.0141). However, the importance of gibbsite is greater than 1:1 clay (0.0302 ± 0.0117 vs 0.0172 ± 0.0041). **B)** *In vitro* growth of *M. abscessus* in the presence of synthetic gibbsite, kaolin and halloysite. **C)** *In vitro* growth of *M. chimera* in the presence of synthetic gibbsite, kaolin, or halloysite. **D)** *In vitro* growth of *M. abscessus* in the presence of Hawai'i soil. **E)** *In vitro* growth of *M. chimaera* in the presence of Hawai'i soil. *** $p < 0.001$, **** $p < 0.0001$.

Figure 3
Glickman and Virdi, *et al*

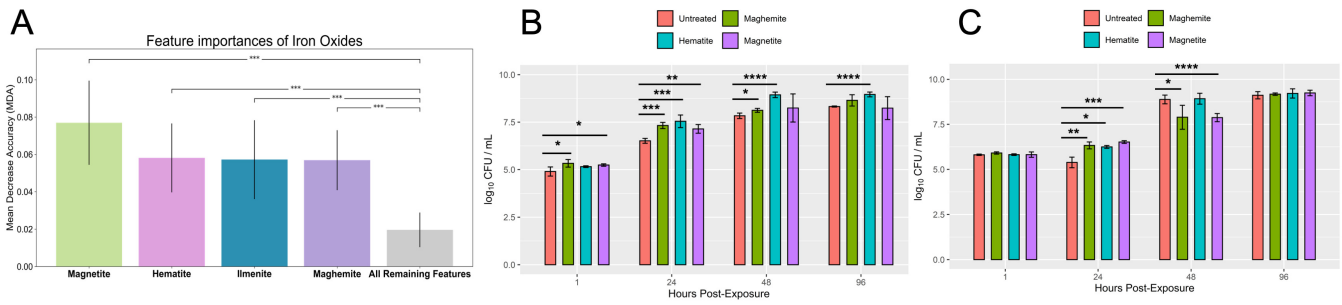

Figure 4. Impact of iron minerals on the *in vitro* growth of native Hawai'i environmental NTM isolates. A) Distribution of iron oxide mean decrease in accuracy across 1,000 iterations of shuffling. The lowest iron oxide mineral (maghemite) is greater than the average of all remaining features suggesting iron oxide minerals are important for NTM growth (0.0569 ± 0.0160 vs 0.0196 ± 0.0092). Magnetite is of greater importance than maghemite or hematite (0.0770 ± 0.0226 vs 0.0569 ± 0.0160 and 0.0581 ± 0.0185. **B)** *In vitro* growth of *M. abscessus* in the presence of synthetic maghemite, magnetite, and hematite. **C)** *In vitro* growth of *M. chimaera* in the presence of synthetic maghemite, magnetite, and hematite. * $p < 0.05$, ** $p < 0.01$, *** $p < 0.001$, **** $p < 0.0001$.

Figure 4
Glickman and Virdi, *et al*

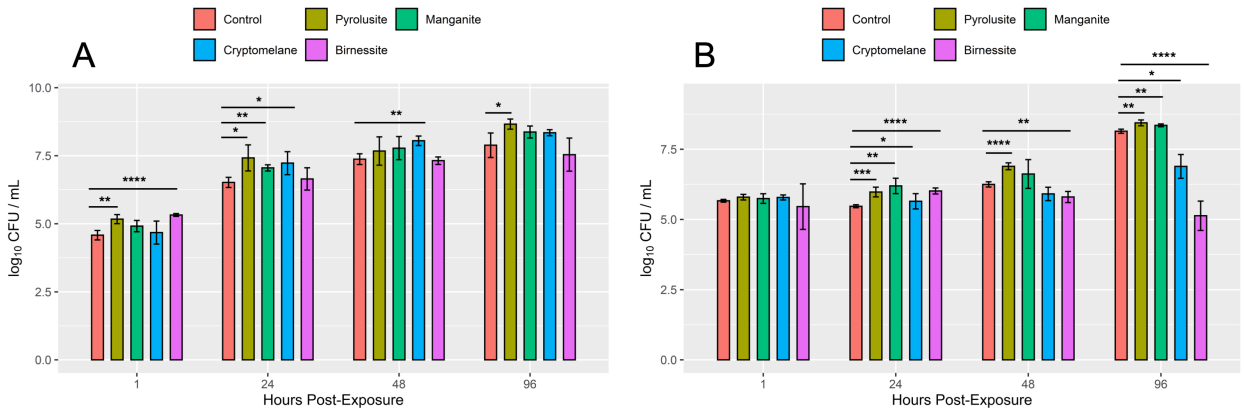

Figure 5. Impact of a manganese compound on the *in vitro* growth of native Hawai'i environmental NTM isolates. *In vitro* growth of *M. abscessus* **(A)** or *M. chimaera* **(B)** in the presence of synthetic manganese minerals. * $p < 0.05$, ** $p < 0.01$, *** $p < 0.001$, **** $p < 0.0001$.

Figure 5
Glickman and Virdi, *et al*

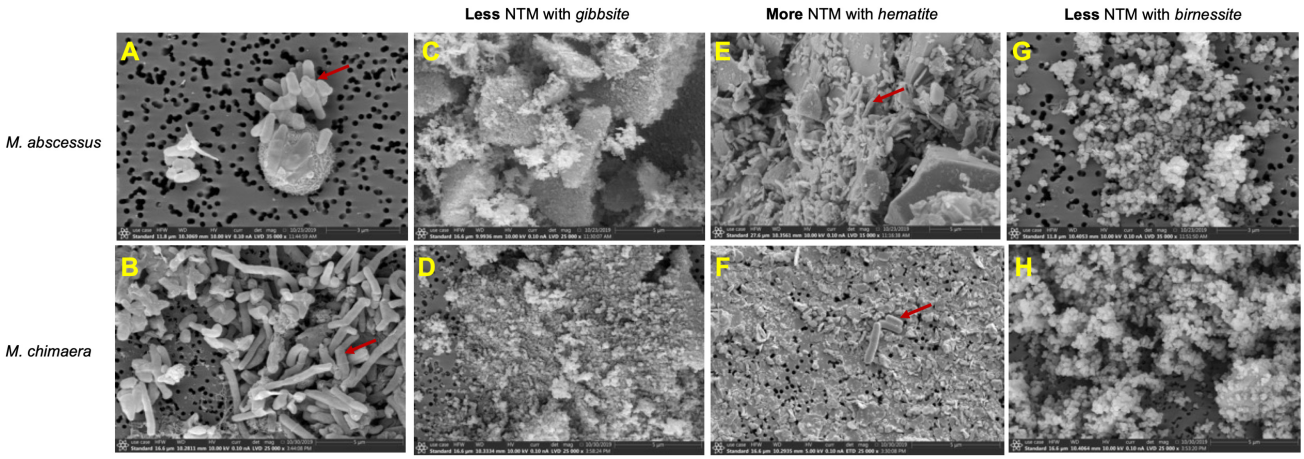

Figure 6. Scanning electron microscope images of environmental NTM isolates grown in the presence of gibbsite, hematite, and birnessite. A-B) *M. abscessus* (3 μm) and *M. chimaera* (5 μm) in the absence of soil minerals. **C-D)** *M. abscessus* and *M. chimaera* in the presence of gibbsite. **E-F)** *M. abscessus* and *M. chimaera* in the presence of hematite. **G-H)** *M. abscessus* and *M. chimaera* in the presence of birnessite. Red arrows indicate the NTM bacilli.

Figure 6
Glickman and Virdi, *et al*